

# Nuclear Response Functions with Realistic Interactions

H. S. Köhler

<sup>1</sup> Physics Department, University of Arizona, Tucson, Arizona 85721, USA

## I. INTRODUCTION

Response functions, the response of a many-body system to an external perturbation is instrumental in our understanding of the properties and interactions involved in the excitations of the system. In the study of nuclear systems these response functions are of particular interest when it comes to calculate the mean free path and absorption of e.g. neutrinos in a neutron gas [1, 2], a subject of interest in astrophysical studies.[3, 4]

They have been the subject of many publications. Nearly all reported calculations use the "HF+RPA" method with Skyrme and/or Gogny effective forces. [5–17] This method ignores the pre-existing correlations in the nuclear medium. But nuclei are strongly correlated many body systems. It is however not trivial to include the effect of these correlations. Simply dressing nucleon-propagators with self-energies leads to inconsistencies. Baym and Kadanoff [18] showed that appropriate vertex corrections are also necessary to guarantee the preservation of the local continuity equation for the particle density and current in the excited system. This in turn implies the satisfaction of the important energy-weighted sum-rule.

These issues were investigated in detail in a previous work.[19] A local interaction, independent of relative momentum, was used which allowed for a proof and test of relations, such as the sum-rule. This interaction also made it possible to use an existing 2-time Kadanoff-Baym computer-code. This work served to illustrate the importance of including correlations of the medium.

Although the properties of the potential were adjusted to comply with known Landau parameters, it was still deficient, e.g. being independent of relative momentum, a known important property of effective interactions in nuclei. Response calculations including the effect of in-medium correlations but with a *realistic* interaction is called for. Our choice of interaction is discussed below. (Section 2). Section 2.1 introduces our choice: Separable interactions constructed by inverse scattering. In Section 2.2 these interactions are used in Brueckner calculations .and in Section 2.3 in Green's function calculations of nuclear matter. Our linear response equations are shown in Section 3. with a discussion of the effective mass in section 3.1 Numerical results are shown in Section 4 with the HF+RPA in Sect 4.1 and correlations included in Section 4.2. A summary and some conclusions are found in Section 5.

## II. NN INTERACTIONS

The known NN-interaction has a short-ranged repulsive component with high energy momentum representation. But the collisions in a nucleus are typically of low energy, of the order of the fermi-momentum. A major breakthrough in our understanding of nucleon interactions in a nucleus is a realisation that these low-energy interactions can (with some caution) be represented by a low energy 'version' of the interaction derived either by renormalising a high energy version as in  $V_{low-k}$  or by EFT power-counting methods.

An important requirement of any realistic NN-potential model is that it reproduces 'free', momentum dependent scattering phase-shifts. A low energy version of the NN interaction can then be defined by a cutoff in momentum space with the requirement that physical quantities, such as the phase-shifts are reproduced up to this cut-off. The practical impact of this low-energy NN interaction is that it allows for a perturbative calculation of nuclear properties [20, 21], as opposed to a typical Brueckner ladder

---

<sup>1</sup> e-mail:kohler@physics.arizona.edu

summation to all orders. Modern realistic low-energy potential of this ‘type derived by EFT methods or  $V_{low-k}$  are available.

Present computer (and programming) limitations prohibits the detailed complexity of these modern nucleon-nucleon interactions for response calculations. It does however seem reasonable that the NN-potential of choice should be realistic in the sense that it reproduces scattering data and that it adequately reproduces the binding energy of nuclear matter as well as mean field data such as effective mass etc to the extent that they are known and affect the outcome of the calculation of interest.

In some previous publications on response functions we used a local Gaussian potential, used in earlier 2-time Kadanoff-Baym calculations. This choice was made partly because of the theory of response such as the energy weighted sum rule could be well documented within this frame work. Another reason for that choice was that the existing 2-time program was designed for local interactions only.[22] Other authors used Gogny or Skyrme interactions for response calculations typically by the HF+RPA method, e.g. [5, 6].

It is however desirable to use a more realistic interaction, realistic in the sense defined above, while still allowing a reasonable computing effort. A 2-body interaction that satisfies these requirements is derived by a purely phenomenological approach, inverse scattering.

See following section for details.

### A. Separable NN interaction.

For the response calculations shown below we are using non-local separable potentials constructed by an inverse scattering method. [23–27]. It

Historically the first separable potential was constructed by Yamaguchi [28]. A well-known attractive feature of such a potential is that it is easier to utilize in many-body calculations since equations are simplified as for example in the context of the Faddeev equations. That was for example the reason for developing a separable version of the Paris potential.[29]

One can in general construct an infinite number of NN interactions which are phase shift equivalent i.e. which fit the on-shell properties of the scattering matrix, but may have different off-shell behaviors [30] Another attractive feature in addition to the one mentioned above is however that one can adjust the off-shell components while keeping the on-shell intact by increasing the rank. Unlike the on-shell the off-shell is however not readily available experimentally, other than indirectly from deuteron data for example as in ref..[26] One may of course also make adjustments to agree with data from some realistic *ab-initio* interaction, as in the afore-mentioned separable Paris potential.

A potential derived by inverse scattering can be termed realistic since it fits the NN phase shifts at any given laboratory energy, although not termed *ab-initio* in the sense that it does not stem from an underlying theory of strong interactions. Its authenticity is further supported by results of binding energy calculations being (almost) identical to those of the Bonn-B potential, in particular as regards the contribution from S-states.[26] The triton binding energy as well as the n-D scattering length was also well reproduced.[31].

For reasons of simplicity in this first presentation of our method, we will include only the S-states (singlet and triplet) and neglect the tensor coupling.

The separable potential will be a function of the momentum cut-off  $\Lambda$  up to which the phase shifts are fitted. Below we show some results of second order (and Brueckner) calculations that lead us to choose  $\Lambda = 2 \text{ fm}^{-1}$  for the response calculations. This together with ignoring the coupling to  ${}^3D_1$  states allows us to use rank one separable potentials for the  ${}^1S$  and  ${}^3S$  states respectively. This rank one potential has the simple form:

$$V_{\Lambda_{\text{cut}}}(k, k') = \lambda v(k)v(k') \quad (1)$$

where  $\lambda = \pm 1$  and  $v(k)$  is the numerical potential form factor which depends on scattering phase-shift via the relation:

$$v^2(k) = -\lambda \frac{(4\pi)^2}{k} \sin \delta(k) |D(k^2)|, \quad (2)$$

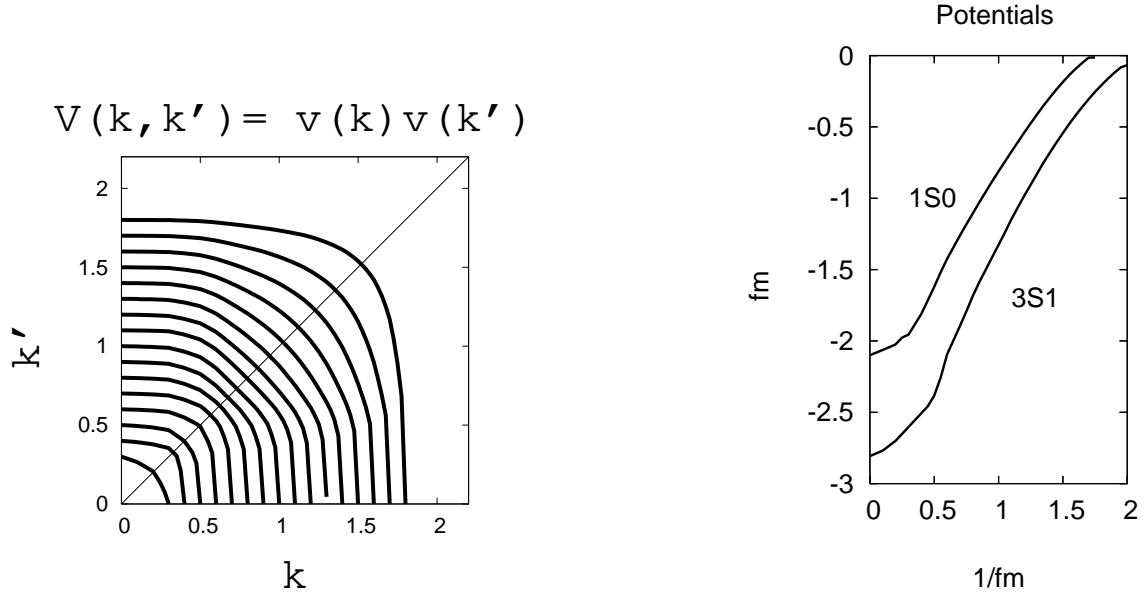


FIG. 1. On the left is shown a contourplot of the separable  ${}^1S_0$  potential with cut-off  $\Lambda = 2 \text{ fm}^{-1}$  that is used in calculations shown below. On the right is shown the diagonal elements of both the  ${}^1S_0$  and the  ${}^3S_1$  potential.

As in previous works [26, 31, 32] we choose to use the phase shifts  $\delta(k)$  from ref. [33]. The function  $D(k^2)$  is defined by:

$$D(\omega) = \frac{\omega + E_B}{\omega} \exp \left[ \frac{2}{\pi} \int_0^\infty \frac{k' \delta(k')}{\omega - k'^2} dk' \right], \quad (3)$$

with the argument  $\omega$  being in general complex and the parameter  $E_B$  standing for energy of the bound state in a specific channel. In our case  $E_B = 0$  since the tensor force is not included and none of the channels has a bound state.

A potential is of course not fully defined by fitting to some phaseshifts. As pointed out above there are an infinite number of solutions to that problem. But as also pointed out above, the contribution to the binding energy of nuclear matter duplicates that of the Bonn-B potential, which is a test of off-diagonal (off-shell) components of the interaction. This is also exhibited by Figs below. Fig. 1 shows a contourplot (left frame) of the separable  ${}^1S_0$  potential used in the calculations of response functions shown below. The right frame shows the diagonal part  $V(k, k) = v(k)v(k)$  of the same potential. The potential is calculated from eqs above with a cut-off  $\Lambda = 2 \text{ fm}^{-1}$ . These results are comparable with the similar display in ref. [20] (Figs 3 and 17) of the  $V_{low-k}$  interaction. Both interactions are momentum-dependent i.e. non-local. The overlap between the two, the  $V_{low-k}$  and the separable is compelling. Note however that this observation refers only to the  ${}^1S_0$  state.

The similarity can be understood by the following: The  $V_{low-k}$  interaction is analogous to that defined by the separation method due to Moszkowski and Scott (MS) [34] as shown by Holt and Brown [35]. The formal difference is that the former as well as our separable potential is defined by a cut-off in momentum-space while the latter by a cut-off in coordinate-space. We point out that the S-state component of a local interaction is non-local although not (necessarily) separable. (See e.g. ref. [36]). The MS-potential is zero within a separation distance  $d \sim 1 \text{ fm}$ , and thus represented by a hollow shell. In the limit of approximating this potential by a 'hard' shell at some distance  $d_{eff}$  this potential is local but the S-state component of this potential is separable. [37] A Gaussian separable potential was used in ref. [38] as an approximation of the MS-potential with (almost) identical overlap. It was there used in a Brueckner calculation of  ${}^{16}\text{O}$  in a Harmonic Oscillator basis.

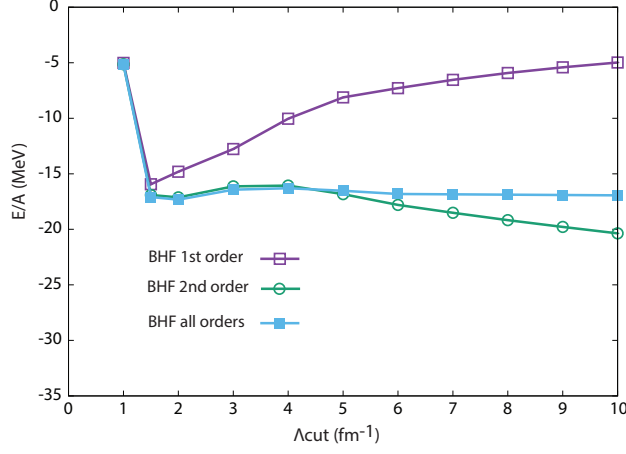


FIG. 2. Nuclear matter energy per particle as a function of momentum cut-off  $\Lambda_{\text{cut}}$  for indicated orders of the interaction, including  $^1S_0$  and  $^3S_1$  channels only.

### B. Nuclear Matter by Brueckner theory.

Using the formalism above we construct separable potentials for momentum cut-offs ranging from  $\Lambda = 1 \text{ fm}^{-1}$  up to  $\Lambda = 10 \text{ fm}^{-1}$  ( including only the  $^1S_0$  and  $^3S_1$  channels ) and we perform Brueckner calculations for symmetric infinite nuclear matter. Table I. shows total energies as a function of  $\Lambda$  in first, second and all orders of the interaction. Fig. 2 displays the same data. The fermi-momentum is  $k_F = 1.25 \text{ fm}^{-1}$ . One sees that the second order calculation produces results almost identical with

TABLE I. Nuclear matter energies in MeV at several orders as a function of the parameter  $\Lambda$ .

$\Lambda \text{ (fm}^{-1}\text{)}$	1 <sup>st</sup> order	2 <sup>nd</sup> order	all orders
1	-5.02	-5.14	-5.16
1.5	-15.94	-16.91	-17.09
2	-14.81	-17.12	-17.33
3	-12.77	-16.13	-16.43
4	-10.04	-16.06	-16.30
5	-8.12	-16.83	-16.53
6	-7.29	-17.80	-16.82
7	-6.54	-18.51	-16.85
8	-5.92	-19.17	-16.88
9	-5.41	-19.78	-16.91
10	-4.98	-20.36	-16.94

the all orders calculation for cutoffs  $\Lambda$  ranging from  $\sim 1 \text{ fm}^{-1}$  up to  $5 \text{ fm}^{-1}$ . We conclude that the separable interaction is soft enough that even at cutoffs as large as  $5 \text{ fm}^{-1}$  the second order calculation is a good approximation. Only the  $^1S_0$  and the  $^3S_1$  partial waves are included and the tensor force is also neglected. Previous results [26] show that contributions of higher angular momentum states almost cancel out; the main contributions come from the S-waves. It is of course well-known that including the tensor force is vital for the saturation of nuclear matter. And so is the short-ranged correlations that are not included when the cut-off is less than  $\sim 2\text{-}3 \text{ fm}^{-1}$ . [32]

The main purpose here is however to establish the usefulness of the low-energy version of the separable potentials (calculated by inverse-scattering) for response-calculations at *normal* nuclear matter density.

The effects of the tensor interaction in the calculation of response functions within the two-time approach will be investigated in subsequent publications.

The results above show that with the S-states to second order together with a cut-off  $\Lambda = 2 \text{ fm}^{-1}$  gives a binding energy of 17.12 MeV/A compared to 17.33 MeV/A in an all order summation. The  $2 \text{ fm}^{-1}$  cut-off allows us to use a rank one separable potential.[26] This will be the choice of interaction in the calculations to follow below. Correlations in the response calculations will be included by second order self-energies.

### C. Nuclear Matter with 2-time Green's functions.

The calculation of response functions follows the methods used in earlier work, time evolving Green's functions by Kadanoff-Baym equations. [22, 39] The Green's functions are separated into a spatially homogeneous part  $G_{00}(t, t')$  and a linear response part  $G_{10}(t, t')$ . Green's functions  $G_{00}(t = 0, t' = 0)$  are constructed for an uncorrelated fermi distribution of specified density and temperature. The  $G_{00}$  functions are then time-evolved (for typically 10 fm/c) with the chosen selfenergies until fully correlated. Selfenergies are calculated to second order with the separable  $^1S$  and  $^3S$  interactions specified above.

The KB-equations for the propagation of these  $G_{00}$  functions as well as numerical methods for solution has already been shown in previous works (e.g. [40]), but included below for completeness.

(summation over  $m = 0, 1$  and integrations over  $\bar{t}$  from  $-\infty$  to  $+\infty$  is implied):

$$\left(i \frac{\partial}{\partial t} - \frac{p^2}{2m} - \Sigma_{00}^{HF}(p, t)\right) G_{00}^{\gtrless}(\mathbf{p}, t, t') = (\Sigma_{00}^{\gtrless}(\mathbf{p}, t, \bar{t}) - \Sigma_{00}^{\lessgtr}(\mathbf{p}, t, \bar{t})) G_{00}^{\gtrless}(\mathbf{p}, \bar{t}, t') - \Sigma_{00}^{\gtrless}(\mathbf{p}, t, \bar{t}) (G_{00}^{\gtrless}(\mathbf{p}, \bar{t}, t') - G_{00}^{\lessgtr}(\mathbf{p}, \bar{t}, t')) \quad (4)$$

$$\left(-i \frac{\partial}{\partial t'} - \frac{p'^2}{2m} - \Sigma_{00}^{HF}(p, t')\right) G_{00}^{\gtrless}(\mathbf{p}, t, t') = (G_{00}^{\gtrless}(\mathbf{p}, t, \bar{t}) - G_{00}^{\lessgtr}(\mathbf{p}, t, \bar{t})) \Sigma_{00}^{\gtrless}(\mathbf{p}, \bar{t}, t') - G_{00}^{\gtrless}(\mathbf{p}, t, \bar{t}) (\Sigma_{00}^{\gtrless}(\mathbf{p}, \bar{t}, t') - \Sigma_{00}^{\lessgtr}(\mathbf{p}, \bar{t}, t')) 1 \quad (5)$$

The past (known) versions of the two-time code limits the calculation of self-energies  $\Sigma^{\gtrless}$  to the use of an interaction that is local (in coordinate space), i.e. momentum independent. A new version of the KB-code has now been developed for the separable potentials with the  $|\Sigma_{00}$  selfenergies given by:

$$\Sigma_{00}^{HF}(\mathbf{p}, t) = i \sum_{\mathbf{p}', \mathbf{j}} G_{00}^{\lessgtr}(\mathbf{p} - \mathbf{p}', t, t) \lambda v_j^2(p') \quad (6)$$

and

$$\Sigma_{00}^{\gtrless}(\mathbf{p}, t, t') = i \sum_{\mathbf{p}_1, \mathbf{p}_2, \mathbf{j}} G_{00}^{\lessgtr}(\mathbf{p}_1, t, t') G_{00}^{\gtrless}(\mathbf{p}_2, t, t') G_{00}^{\gtrless}(\mathbf{p} + \mathbf{p}_2 - \mathbf{p}_1, t, t') \times v_j^2(2\mathbf{p}_1 - \mathbf{p} - \mathbf{p}_2) v_j^2(\mathbf{p} - \mathbf{p}_2) \quad (7)$$

where the index  $j = 1, 2$  refers to the two S-states.

A diagrammatic representation of the self-energy  $\Sigma_{00}$  is shown in Fig. 5.

Fig. 3 shows the separate energies, (kinetic, potential and total) as a function of time in a calculation with the separable  $^1S_0$  and  $^3S_1$  interactions defined above. The cutoff  $\Lambda = 2 \text{ fm}^{-1}$ .

The initial state is here a zero-temperature fermi-distribution, uncorrelated. The fermimomentum in this and in results below are for symmetric nuclear matter with  $k_f = 1.25 \text{ fm}^{-1}$ . The equations are time-stepped until system is fully correlated. The time-scale starts for convenience at  $t = -10 \text{ fm}/c$  with the system considered fully correlated at  $t = 0$  with a correlation time  $t_c = 10 \text{ fm}/c$ . [41] The external perturbation is applied as a pulse centered at  $t = 0$ . All energies are shifted to zero at  $t = -10$ . This is to better show the change in energies from the uncorrelated to the correlated state. The total energy (kinetic+potential) is constant in time, which is the result of conserving approximations for the selfenergies. [18] The interaction (potential) energy  $E_{pot}$  includes both the mean field  $E_{mf}$  and a

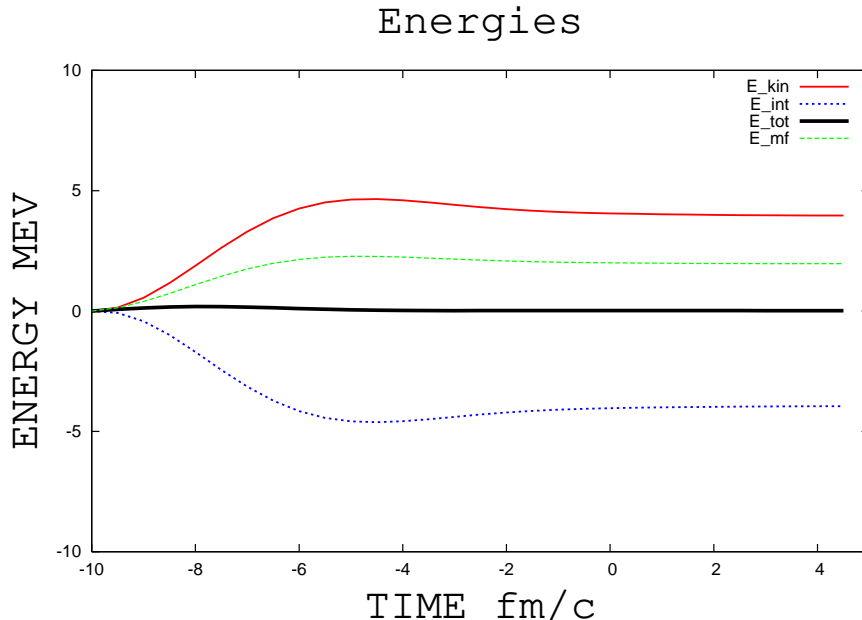


FIG. 3. Energies as a function of time starting at  $t = -10$  fm/c. Results shown are from top to bottom: kinetic (red online), mean field (green online), total (black online) and potential (blue online) energies. Energies are shifted to energy = zero at time  $t = -10$ . See text for further details.

'correlation' energy  $E_{corr}$ . The initial ( $t = -10$ ) kinetic (same as total) and mean field energies are 19.4 and  $-37.4$  MeV respectively.

At the end of the run the kinetic, interaction and mean-field energies have changed by  $+4.0a$ ,  $-4.0$  and  $+2.0$  MeV respectively and the correlation energy (the difference between the interaction and mean-field energies)  $E_{corr} = 6.0$  MeV. It might seem that this energy should be comparable with the second order contribution in Section 2.2, the difference between the first and second order results found in Table 1, which is seen to be 2.31 MeV, a difference of almost a factor of three. There are several reasons for this apparent "discrepancy". One is the effect of the mean field, which is a consequence of the redistribution in momentum-space shown below in Fig. 4. Neglecting the mean field in each of the two calculations the Brueckner gives  $-4.1$  MeV for the second order Born contribution while the KB gives  $-8.9$  MeV i.e. a factor of  $\sim 2$ . A factor of exactly 2 was already demonstrated to be the exact value to be expected in the Levinson (and the extended quasiparticle) approximation of the collision term.[41, 42]. It is associated with the increase in kinetic energy (see Figs 3 and 4) with the KB method.

Fig. 4 shows the correlated distribution in momentum space. It is seen to compare reasonably well with the many previously published results at the fermi-surface. (e.g. ref.[22]). The depletion of interior states is however appreciably less. This is because of cut-off of the large momenta (short ranged) as well as the neglect of the tensor-component in these calculations.

### III. LINEAR RESPONSE WITH THE SEPARABLE NN-POTENTIAL.

The formalism associated with the calculation of the response-function using the 2-time KB- method has been shown in previous works [22, 39].

Eqs (4) and (5) showed the time-evolution of the Green's functions  $G_{00}^>$  for the unperturbed nuclear system. At a correlation time  $t = t_c$ , ( $t = 0$  in Fig.3) this system is 'hit' by an external potential  $U(\mathbf{q}, t) = U_0(t)\delta_{\mathbf{q}, \mathbf{q}_0}$  that results in collective excitations. These excitations are contained in Green's functions  $G_{10}^>$ , obeying the equations (summation over  $m = 0, 1$  and integrations over  $\bar{t}$  from  $-\infty$  to  $+\infty$  is implied):

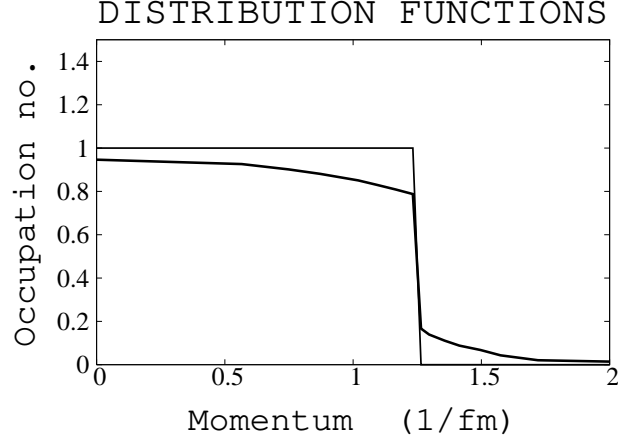


FIG. 4. Shown here is the zero temperature Fermi-distribution (top curve) and the correlated distribution from the second-order selfenergy calculations.

$$\begin{aligned} \left( i\hbar \frac{\partial}{\partial t} - \epsilon_{\mathbf{k}+\mathbf{q}_0} \right) G_{10}^{\lessgtr}(\mathbf{k}t t') &= U_0(t) G_{00}^{\lessgtr}(\mathbf{k}t t') + \Sigma_{1m}^{HF}(\mathbf{k}t) G_{m0}^{\lessgtr}(\mathbf{k}t t') \\ &+ \Sigma_{1m}^R(\mathbf{k}t \bar{t}) G_{m0}^{\lessgtr}(\mathbf{k} \bar{t} t') + \Sigma_{1m}^{\lessgtr}(\mathbf{k}t \bar{t}) G_{m0}^A(\mathbf{k} \bar{t} t') \end{aligned} \quad (8)$$

and

$$\begin{aligned} \left( -i\hbar \frac{\partial}{\partial t'} - \epsilon_{\mathbf{k}} \right) G_{10}^{\lessgtr}(\mathbf{k}t t') &= U_0(t') G_{11}^{\lessgtr}(\mathbf{k}t t') + G_{1m}^{\lessgtr}(\mathbf{k}t t') \Sigma_{m0}^{HF}(\mathbf{k}t') \\ &+ G_{1m}^R(\mathbf{k}t \bar{t}') \Sigma_{m0}^{\lessgtr}(\mathbf{k} \bar{t} t') + G_{1m}^{\lessgtr}(\mathbf{k}t \bar{t}') \Sigma_{m0}^A(\mathbf{k} \bar{t} t') \end{aligned} \quad (9)$$

A diagrammatic representation of the self-energies is shown in Fig. 5. (See also ref. [22] for a more complete exhibition.) We distinguish between three contributions to the self-energy  $\Sigma_{10}^{\lessgtr}$  corresponding to the three second order diagrams shown in Fig 5 and write

$$\Sigma_{10}^{\lessgtr}(\mathbf{p}, t, t') = \sum_{n=1,3} \Sigma_{(n)}^{\lessgtr}(\mathbf{p}, t, t')$$

with

$$\begin{aligned} \Sigma_{(1)}^{\lessgtr}(\mathbf{p}, t, t') &= i \sum_{\mathbf{p}_1, \mathbf{p}_2} G_{10}^{\lessgtr}(\mathbf{p}_1, t, t') G_{00}^{\lessgtr}(\mathbf{p}_2, t, t') G_{00}^{\lessgtr}(\mathbf{p} + \mathbf{p}_2 - \mathbf{p}_1, t, t') \times \\ &v^2(2\mathbf{p}_1 - \mathbf{p} - \mathbf{p}_2) v^2(\mathbf{p} - \mathbf{p}_2) \end{aligned} \quad (10)$$

$$\begin{aligned} \Sigma_{(2)}^{\lessgtr}(\mathbf{p}, t, t') &= i \sum_{\mathbf{p}_1, \mathbf{p}_2} G_{00}^{\lessgtr}(\mathbf{p}_1, t, t') G_{00}^{\lessgtr}(\mathbf{p}_2, t, t') G_{10}^{\lessgtr}(\mathbf{p} + \mathbf{p}_2 - \mathbf{p}_1, t, t') \times \\ &v(2\mathbf{p}_1 - \mathbf{p} - \mathbf{p}_2) v(2\mathbf{p}_1 - \mathbf{p} - \mathbf{p}_2 + \mathbf{q}_0) v(\mathbf{p} - \mathbf{p}_2) v(\mathbf{p} - \mathbf{p}_2 + \mathbf{q}_0) \end{aligned} \quad (11)$$

$$\begin{aligned} \Sigma_{(3)}^{\lessgtr}(\mathbf{p}, t, t') &= i \sum_{\mathbf{p}_1, \mathbf{p}_2} G_{00}^{\lessgtr}(\mathbf{p}_1, t, t') G_{10}^{\lessgtr}(\mathbf{p}_2 - \mathbf{q}_0, t, t') G_{00}^{\lessgtr}(\mathbf{p} + \mathbf{p}_2 - \mathbf{p}_1, t, t') \times \\ &v^2(2\mathbf{p}_1 - \mathbf{p} - \mathbf{p}_2) v^2(\mathbf{p} - \mathbf{p}_2) \end{aligned} \quad (12)$$

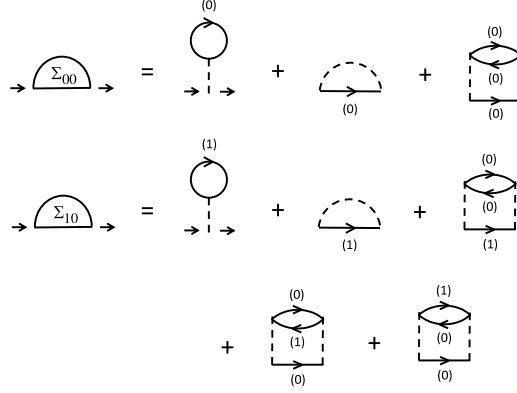


FIG. 5. Diagrams representing contributions to the self energy in the Kadanoff-Baym equations to zeroth order ( $\Sigma_{00}$ ) and first order ( $\Sigma_{10}$ ) in the external perturbation  $U$ . The solid (dashed) lines are correlated Green's functions NN interactions). The number near each Green's function line gives the order in  $U$  of that line.

where

$$G_{10}^>(\mathbf{k}, t, t') \equiv G_{10}^>(\mathbf{k} + \mathbf{q}_0, t; \mathbf{k}, t') \quad (13)$$

The retarded and advanced parts above are given by

$$\Sigma_{10}^{R/A}(\mathbf{p}, t, t') = \pm\theta(\pm(t - t'))[\Sigma_{10}^>(\mathbf{p}, t, t') - \Sigma_{10}^<(\mathbf{p}, t, t')] \quad (14)$$

Results of calculations are shown below following a discussion of the effective mass.

### A. Effective mass

The effective mass plays a very important role in the theory of response-functions. It determines a mean energy of the excitation as is evident from the energy weighted sum-rule: It will be seen below that it also affects the width of the response function.

$$\int \omega S(\omega, q_0) d\omega = \frac{q_0^2}{2m^*} \quad (15)$$

We are in particular interested in the response in the long wave-length limit with excitations close to the fermi-surface. The effect of the external perturbation will depend on the energy-spectrum  $e(k)$  out of which the particles are excited, conveniently expressed in terms of the effective mass  $m^*$  with ( $\hbar = 1$ )

$$e(k) = \frac{k^2}{2m} + U(k) = U(0) + \frac{k^2}{2m^*(k)}$$

The effective mass will, as indicated, in general be a function of  $k$  with  $m^*(k_F)$  being the effective mass of interest here. It has been the subject of many calculations and discussions since early works on the Landau theory and nuclear many body problem in general. (see e.g. [43]). Of particular interest for our present work is that of Bäckman [44] and Sjöberg [45], related to Landau theory. In the calculations presented below we are defining an 'effective' effective mass  $m^{**}$  from inverting eq. 15.

$$m^{**} = \frac{q_0^2}{2 \int \omega S(\omega, q_0) d\omega} \quad (16)$$



This relies on the fact that our equations do satisfy the energy sum-rule. This was tested and verified by replacing the Hartee- Fock field  $\Sigma_{00}^{HF}$  below in eqs (8) and (9) by an effective mass approximation.

The definition of  $U(k)$  or equivalently  $e(k)$ , is evidently of utmost importance. We are here concerned with excitations due to an external perturbation and the definition relevant for the present work is then

$$e(k) = \frac{dE}{dn_k} \quad (17)$$

i.e. the removal energy. In Brueckner theory this would include terms to first order in the Brueckner  $K$ -matrix as well as the higher order rearrangement terms. There are numerous publication and discussions in the literature on this subject matter. The third order term  $U^{(3)}$  is related to the depletion factor  $\kappa$  by

$$U^{(3)} = -\kappa U^{(1)}.$$

Köhler and Moszkowski [32] evaluated contributions to this depletion factor for eight of the most important spin-isospin states for our separable potential with  $1.6 < \Lambda < 9.8 \text{ fm}^{-1}$ . The results showed a strong dependence on the cut-off  $\Lambda$ . For the largest cut-off considered,  $\Lambda = 9.8 \text{ fm}^{-1}$  they found  $\kappa = .175$  for a density with  $k_F = 1.35 \text{ fm}^{-1}$ . For  $\Lambda = 2.6 \text{ fm}^{-1}$  (the closest to or chosen value  $\Lambda = 2.0$ ) they found  $\kappa = 0.124$ . The largest contribution was for the coupled  ${}^3S_1$ - ${}^3D_1$  states which we do not include at present. It does however seem appropriate to here adopt the value  $\kappa = .17$ .

The second order term  $U^{(2)}$  stems from the change in Pauli-blocking upon removal of a nucleon. The significance of this term was discussed early on by Brueckner et al [46] and later in refs. [36, 47] It is strongly momentum-dependent and thus quite important as regards the effective mass. An increase of the effective mass near the fermisurface by  $\sim 0.15$  compared to that for deeper states is expected.[43]

The modification (increase) of the effective mass from that given by a first order mean field calculation is of importance for the response calculations. While our first order result yields  $m^* \sim 0.6$  the rearrangement terms increases it to  $m^* \sim 0.8 - 0.9$ . This should be compared with the Landau value close to  $m^* = 1.$ , validated by experimental evidence[48]. We return to the question of the effective mass in the Results section below.

## IV. NUMERICAL RESULTS

The formalism presented above is applied to calculating response functions of symmetric nuclear matter at normal density. To fully appreciate the importance of the various self-energies etc we also show some results of approximations.

### A. HF+RPA

Most published reports on response functions use the HF+RPA method. This implies neglecting all effects of correlations, i.e. all second order self-energies in Fig. 5. while maintaining the mean fields. Our results are shown in Fig. 6, all with  $q_0 = 0.4 \text{ fm}^{-1}$ . The left curve shows the result with the mean field calculated selfconsistently. The 'effective' effective mass  $m^{**}$  is here obtained from eq. (16). The result is  $m^{**} = 0.66$ .

In the two other results the mean field is, as indicated, replaced by an effective mass approximation, which allows us to test and verify the energy sum rule. It also shows the importance of the effective mass as it affects the response, a point emphasized in this paper.

### B. Effect of Correlations

The solid black (right) line in Fig. 7 shows the response function calculated including all self energies i.e with correlated Green's functions as shown by eqs (4) and (5). A comparison with the HF+RPA-result shown in Fig. 6 shows a considerable difference. Part of this difference is related to the difference

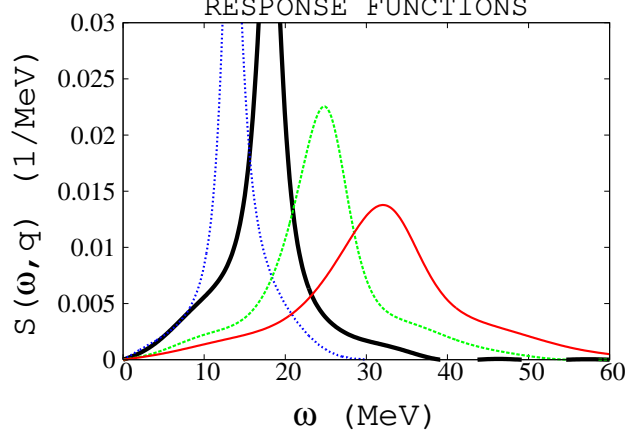


FIG. 6. Response functions with mean-field only; no correlations i.e. by the HF+RPA method. From left to right: The first line (blue online) is with the HF mean field  $\Sigma_{00}^{HF}$  set to zero i.e. with  $m^* = m^{**} = 1$ . The solid black line is with the HF-field calculated with the  $^1S$  and  $^3S$  separable potentials. It relates to an effective mass  $m^{**} = 0.66$ . (See text regarding definition of  $m^{**}$ .) The next, broken line (green online), shows the result with the mean field replaced by an effective mass  $m^* = 0.5$  and the last curve, broken line (blue online), with an effective mass  $m^* = 0.4$ . It is seen that there is not only a shift in energy but also a broadening of the response function when the effective mass decreases. All results are with  $q_0 = 0.4 \text{ fm}^{-1}$ .

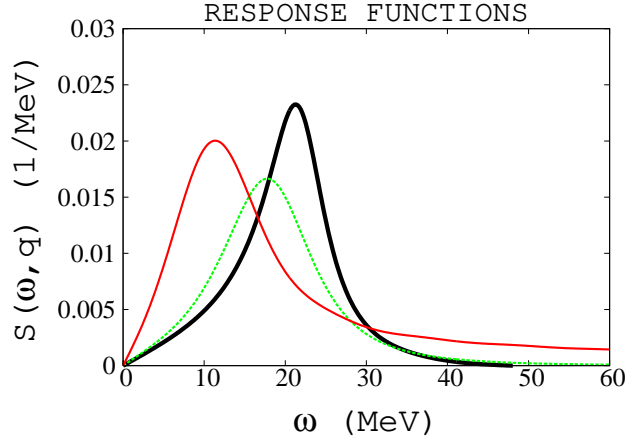


FIG. 7. The full line to the right (black online) shows the response function with all self-energies calculated with self-consistent correlated Green's functions. It relates to an effective mass  $m^{**} = 0.61$ . The left dotted line (red online) shows the result with all self-energies  $\Sigma_{10}^{\leq} \equiv 0$ . (In Fig. 5 denoted by  $\Sigma_{10}$ .) The energy sum rule is here grossly violated. The middle line (green online) neglects correlations between the  $G_{00}$  and  $G_{01}$  Green's functions. (Last two diagrams in Fig.2) See text for further details. All results are with  $q_0 = 0.4 \text{ fm}^{-1}$ .

in effective masses  $m^{**}$ , 0.66 vs 0.61. Including only the second order self-energies  $\Sigma_{00}^{\leq}$  but neglecting the corresponding  $\Sigma_{10}$  terms in eqs (10), (11) and (12), (i.e. neglecting the vertex-corrections) one finds a response-function as shown by the left (red online) curve in Fig. 7. It shows the well-known error in neglecting the vertex-corrections with a gross violation of the sum-rule, eq. (15). Also shown (middle curve green online) is the result when neglecting the contributions shown by eqs (11) and (12). (last two diagrams in Fig. 5).

The importance of the effective mass was already emphasized above in a separate section.. A typical

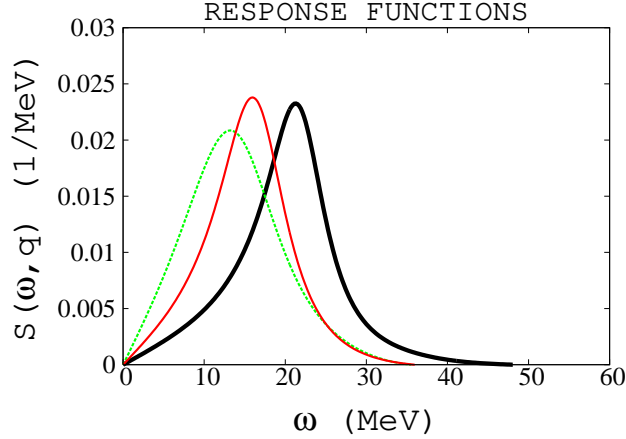


FIG. 8. The full line to the right (black online) shows the response function with all self energies calculated with self-consistent correlated Green's functions. (Same as in Fig 7). The dotted line to the left (green online) shows the result with  $\Sigma_{00}^{HF} \equiv 0$  in the eqs for  $G_{10}$  only. The effective mass is in this case  $m^{**} = 1$ . The dotted line in the middle (red online) was obtained by assuming  $\Sigma_{00}^{HF} \equiv 0$  also in the eqs for  $G_{00}$ , i.e. also with  $m^{**} = 1$ . All results are with  $q_0 = 0.4 \text{ fm}^{-1}$ .

value for Brueckner and similar many-body calculations is  $m^* \sim 0.7$ , consistent with the values shown above. There are however the well-known corrections, (e.g. second and third order 'rearrangement' corrections) that would bring this value up. Landau theory is more compatible with an effective mass close to  $m^* = 1$ . We therefore show in Fig 8 our result for this case. It is obtained by setting  $\Sigma_{00}^{HF} = 0$  with results shown in Fig. 8. The sum-rule is consequently now satisfied with  $m^{**} = 1$ .

## V. SUMMARY AND CONCLUSIONS

A new computer program was designed to time-evolve 2-time Kadanoff-Baym equations with self-energies computed with non-local separable two-nucleon interactions. Previous program was restricted to the use of local interactions only, while it is well known that a realistic representation of effective nuclear forces are indeed non-local i.e. momentum dependent. A local interaction is in momentum=space a function of momentum *transfer* only.

The program was here used for the calculations of response functions for symmetric nuclear matter. The all-important energy weighted sum-rule was found to be well satisfied, validating the integrity of the calculations.

Previous calculations presented in the literature are with few exceptions done in the HF+RPA approximation, i.e. neglecting the effect of correlations in the nuclear medium. These correlations, related to the strong nuclear forces, have been the focus of intense studies since the "birth" of nuclear physics. It has been the purpose of this work to investigate the effect of these correlations on the calculations of nuclear response. There are three separate (although related) effects to be expected. I. The correlations result in a redistribution of occupied states as shown in Fig. 4. II. The selfenergies are complex. This causes a broadening of states in general, while spectral functions of an uncorrelated medium are represented by delta-functions. This broadening is of course the root of the effect labelled by I. But it also causes a broadening of the response functions as seen by comparing the full curves (black online) in Figs. 6 and 7. The third effect relates to the selfenergies  $\Sigma_{10}$ . It is since a long time well known that the introduction of correlations in numerical calculations as done here is not trivial. Selfenergy insertions in propagators have to be accompanied by proper vertex corrections. This is 'automatically' accomplished by the self-energies denoted by  $\Sigma_{10}$  in Fig. 5. Neglecting this term in the calculations result in a gross violation of the sum rule as shown in Fig. 7.

An important factor to consider is also the effective mass. It has been a subject of numerous calcu-

lations and even more discussions in the literature. (See section 3.3 above.) In the context of response it is of course vital because it is as shown above, essential in determining the 'location' of the response along the  $\omega$ -axis. It also affects the width of the response function. As was already discussed in section 3.3, there are numerous corrections that have to be included if a microscopic calculation is implemented. Our calculations above yield a Brueckner (first order) estimate of  $m^*=0.6$  to  $0.7$ . Second and third order corrections may rise this to  $m^* \sim 0.9$ . Empirical data (from experimental spectral densities) suggest a value close to  $m^* = 1.0$ .[\[48\]](#)

The effective mass is also an important factor as regards the energy-weighted sum-rule. It was shown in an earlier work [\[19\]](#) that if all selfenergies were calculated consistently with a *local* interaction the sum -rule is satisfied with  $m^{**} = 1$ . (See above for definition of  $m^{**}$ .) If an external mean field  $\Sigma_{00}$  was added the sum-rule was then satisfied with the effective mass of this external field.

This situation is changed with the non-local interaction. The value of  $m^{**}$  was always found to be that of the chosen, not necessarily consistent, mean field  $\Sigma_{00}$ . It was however also illustrated above that all selfenergies have to be included. The sum-rule would otherwise be (sometimes grossly) violated.

## VI. ACKNOWLEDGEMENTS

I thank Dr George Papadimitriou for help with the nuclear matter calculations and accompanying figures and Prof N.H. Kwong for numerous discussions. I thank The University of Arizona and in particular the Department of Physics for providing office space and access to computer facilities.

- 
- [1] J. Margueron, J. Navarro, P. Blottiau, Phys. Rev.C **70** 028801 (2004).
  - [2] Naoki Iwamoto and C.J. Pethick, Phys. Rev.D **25** 313 (1982).
  - [3] S. Reddy, M. Prakash, J. Lattimer, J. Pons Phys. Rev.C **59** 2888 (1998).
  - [4] A. Sedrakian and A. Dieperink, Phys. Rev.D **62** 083002 (2000).
  - [5] D. Gogny and R. Padjen, Nucl. Phys. A **293** 365(1977)
  - [6] C. Garcia-Recio, J. Navarro, Van Gai Nguyen and L.L. Salcedo, Ann. Phys.(N.Y.) **214** 340 (1992).
  - [7] E. Olsson, P. Haensel and C.J. Pethick, Phys. Rev.C **70** 025804 (2004).
  - [8] J. Margueron, Nguyen Van Giai and J. Navarro, nucl-th/0507053.
  - [9] J. Margueron, J. Navarro and N. Van Giai, Phys. Rev.C **74** 015805 (2006).
  - [10] J. Margueron, J. Navarro and N. Van Giai and P. Schuck, Phys. Rev.C **77** 064306 (2008).
  - [11] Armen Sedrakian and Jochen Keller, nucl-th/1001.0395 Jochen Keller and Armen Sedrakian nucl-th/1205.6902
  - [12] D. Gambacurta, U. Lombardo and W. Zuo, Physics of Atomic Nuclei, **74** 1424 (2011).
  - [13] A. Pastore, M. Martini, D. Davesne, K.Bennaceur, and J. Meyer, Phys. Rev.C **86** 044308 (2012).
  - [14] A. Pastore, D. Davesne and J. Navarro, J. Phys. G **41** 055103 (2014).
  - [15] A. Pastore, D. Davesne and J. Navarro, Phys. Rept. **63** 1 (2015).
  - [16] A. De Pace and M. Martini, Phys. Rev. C **94** 024342 (2016).
  - [17] Takashi Nakatsukasa, nucl-th/1701.01278;
  - [18] Gordon Baym and Leo P. Kadanoff, Phys. Rev. **124** 287 (1961) ; Gordon Baym, Phys. Rev. **127** 1391 (1962).
  - [19] H.S. Köhler and N.H. Kwong, preprint.
  - [20] K. Hebeler, S.K. Bogner, R.J. Furnstahl, A. Nogga and A. Schwenk, Phys. Rev.C **83** 031301 (2011).
  - [21] S. Bogner, R. Furnstahl and A. Schwenk, Progress in Particle and Nuclear Physics **65**, 94 (2010), ISSN 0146-6410.
  - [22] H.S. Köhler and N.H. Kwong, Journal of Physics: Conference Series **6** 012011 (2016)
  - [23] M. Gourdin and A. Martin, Il Nuovo Cimento **6** 757 1957.
  - [24] K. Chadan and P. Sabatier, Inverse Problems in Quantum Scattering Theory, 2nd ed. (New York, Springer, 1992).
  - [25] F. Tabakin, Phys. Rev. **177** 1443 (1969).
  - [26] N.H. Kwong and H.S. Köhler, Phys. Rev.C **55** 1650 (1997).
  - [27] A. Shirokov, J. Vary, A. Mazur and T. Weber, Physics Letters B **644** 33 (2007), ISSN 0370=2693
  - [28] Y. Yamaguchi, Phys. Rev. **95** 1628 (1954).
  - [29] J. Haidenbauer and W. Plessas, Phys. Rev.C **30** 1822 (1984).
  - [30] V. Bargmann, Rev. Mod. Phys. **21** 488 (1949)
  - [31] H.S. Köhler, nucl-th/0907.1539
  - [32] H.S. Köhler and S.A. Moszkowski, nucl-th/0703093
  - [33] R.A. Arndt, L.D. Roper, R.L. Workman and M.W. McNaughton; Phys. Rev.D **45** 3995 (1992).
  - [34] S. A. Moszkowski and B. L. Scott Ann. Phys. (N.Y.) **11** 65 1960.
  - [35] J.W. Holt and G.E. Brown, nucl-th/0408047.
  - [36] H.S. Köhler, Phys. Rev. **137** B1145 (1965).
  - [37] S.A. Moszkowski, Private Communication.
  - [38] H.S. Köhler, Nucl. Phys. **38** 661(1962)
  - [39] N. H. Kwong and M. Bonitz, Phys. Rev. Letters **84** 1768 (2000).
  - [40] H.S. Köhler, N.H. Kwong and Hashim A. Yousif, Comp.Phys.Comm. **123** 123 (1999)
  - [41] H.S. Köhler and K. Morawetz, Phys. Rev.C **64** 024613 (2001).
  - [42] H.S. Köhler and Rudi Malfliet, Phys. Rev.C **48** 1034 (1992).
  - [43] J.P. Jeukenne, A. Lejeune and C. Mahaux, Physics Reports **25** 83 (1976).
  - [44] S.-O. Bäckman, Nucl. Phys. A **120** 593 (1968)
  - [45] O. Sjöberg. Ann. Phys.(N.Y.) **78** 39 (1973).
  - [46] K. A. Brueckner and J. L. Gammel, Phys. Rev. **109** 1022 (1958).

- [47] R. Sartor and C. Mahaux, Phys. Rev.C **21** 1546 (1980).
- [48] G. E. Brown, J.H. Gunn, and P.Gould, Nucl. Phys. **46** 598(1963)